JOURNAL OF MATERIALS SCIENCE 29 (1994) 1159–1168

Laser surface modification of Ti–6Al–4V alloy

O. V. AKGUN, O. T. INAL
New Mexico Institute of Mining and Technology, Department of Materials and Metallurgical Engineering, Socorro, NM 87801, USA

Hardening of Ti–6Al–4V alloy with laser surface melting (LSM) and laser surface alloying (LSA) techniques was attempted. Both LSM and LSA were carried out in a nitrogeneous atmosphere. Niobium, molybdenum and zirconium were used as alloying elements in the LSA. A hardness increase was observed for both LSM and LSA. Maximum hardness was obtained for LSM and zirconium alloy addition. In LSM, hardness increased almost three-fold in comparison to the substrate, which has a Vickers hardness of 350, by the formation of TiN in the region of 100 μm melt depth. Hardness then decreased slowly and reached a minimum of 580 VHN at the maximum melt depth of 750 μm. However, hardness for the zirconium alloy addition was uniform throughout the melted zone. Ageing treatments were performed for all specimens at 450 °C and different ageing times. Hardness measurements and X-ray diffraction were utilized to delineate the features associated with the hardening of the melted zone.

1. Introduction

Titanium and its alloys are known for their specific strength as well as corrosion and fatigue resistance [1]. However, they suffer from low wear and gall resistance which, in turn, limit their use in tribological applications [2].

There are techniques available that increase the surface hardness of titanium alloys through modification of composition or microstructure. Conventional nitriding techniques, such as ion-nitriding, nitrogen gaseous nitriding, salt-bath nitriding and others, utilize the formation of TiN in the surface layer as a result of nitrogen diffusion [3–5]. The thickness of the layer is a function of process temperature, time and nitrogen pressure. However, they all have the disadvantage of requiring high process temperatures and extensive hours of processing.

Ion implantation has recently emerged as a new technique to improve surface hardness of titanium alloys [6–8]. When ion species such as nitrogen, carbon and boron are implanted into surface layers of titanium alloys, they form hard titanium-base metallic compounds such as TiN, TiC and TiB. The thickness of the hardened surface layer, though, is only a few micrometres. Additional disadvantages of ion implantation are the requirements of long processing time and the limitation of specimen sizes.

Laser processing techniques, such as laser surface melting (LSM) and laser surface alloying (LSA), are widely used for surface modification. Improved hardness, corrosion and wear resistance have been observed for ferrous and non-ferrous alloys [9–14]. In addition, laser processing offers more practical working conditions, such as short processing time, unlimited specimen size and easy control of the treated surface thickness. Therefore, in this study, laser surface melting and alloying of Ti–6Al–4V alloy was carried out, in a nitrogeneous atmosphere, to form TiN in the surface layer and thus increase the surface hardness. Molybdenum, niobium and zirconium were used as alloying elements in the second study (LSA) to elucidate the hardness increment associated with this processing as well. These elements are also known to improve high-temperature properties of Ti–6Al–4V alloy. Resulting microstructures were analysed with X-ray diffraction and hardness measurements. Ageing treatments were carried out to introduce further microstructural changes and determine their effect on hardness of the melted and alloyed regions. Processing variables for laser surface treatment will be discussed briefly in the following section, previous to the presentation of the experimental results.

2. Process variables

The key variables that control efficiency of laser surface processing are laser power, beam size, and scan speed; they determine the extent of surface alloying, coating composition and coating thickness. An increasing laser power increases the melt depth, provides uniform mixing in the melted pool, increases the heat affected zone, and increases absorbtivity; however, it also increases surface rippling and the tendency to crack formation in the melted zone. Focusing the laser beam to small diameters provides a high power density that increases melt depth, but decreases the melt width. An increasing scan speed means less interaction time between the laser beam and material, decreases melt width and depth, reduces fluid flow and this, in turn, affects the homogenization of the melted zone, changes the shape of the fusion zone from semicircular to elliptical, decreases surface rippling and, due to high cooling afforded, reduces dentrite arm spacing.

0022–2461

Reflectivity, by the substrate, of the laser beam is also an important variable for the efficiency of the laser processing. Ferrous metals, such as steels, have low reflectivity while non-ferrous metals, such as aluminium and copper, show almost 100% reflectivity. The surface roughness of the substrate material and the wavelength of the laser beam also control the reflectivity of the laser beam. An increasing surface roughness increases reflectivity, while reflectivity decreases with decreasing wavelength of the laser beam. However, when the surface of the material reaches its melting temperature, reflectivity becomes independent of the above-mentioned variables and approaches zero.

Additionally, in surface alloying, the coating of the alloying element must be made thick enough to ensure the presence of the desired alloy composition in the melted zone and to compensate for the material losses due to vaporization during the interaction with the high-power laser beam.

3. Various possible phases of Ti–6Al–4V alloy

3.1. Equilibrium phases

The equilibrium phases of Ti–6Al–4V alloy at ambient temperature are α and β. The presence of aluminium in Ti–6Al–4V alloy extends α-phase and raises the β/(α + β) transus. However, the addition of vanadium, which is a β stabilizer, extends the α + β region by lowering the (α + β)/β transus. The equilibrium phases of ternary Ti–6Al–4V alloy at various temperatures are shown in Fig. 1. At high temperatures the β-phase is stable, but as the temperature decreases, the β content of the microstructure decreases as well. When the temperature is lowered to 600 °C, β-phase disappears and alloy composition falls on the α-solvus line; therefore, the Ti–6Al–4V ternary alloy is termed near-α, α + β alloy.

3.2. Non-equilibrium phases

Ti–6Al–4V is a heat-treatable alloy, therefore, a wide range of heat-treatment techniques, such as quenching and ageing, can be applied to produce different microstructures. The non-equilibrium phases referred to herein represent the final states of these heat treatments. Rapid quenching from the β field, through the α + β region, causes martensitic transformation [16]. The resulting martensitic morphologies can be massive or acicular martensite. Stress-induced martensitic transformation is also observed for β-stabilized titanium alloys. In this case, metastable β-phase transforms to martensite under the application of mechanical stresses. Slow cooling from the β field, on the other hand, provides enough time for α-phase nucleation and growth to occur, causing the characteristic Widmanstätten structure [17].

4. Strengthening of titanium alloys

The strengthening of titanium alloys can be considered in terms of solid solution or microstructural strengthening. A wide range of microstructures, and associated mechanical properties, can be achieved as a result of heat treatment of near-α, α + β alloy (i.e. Ti–6Al–4V).

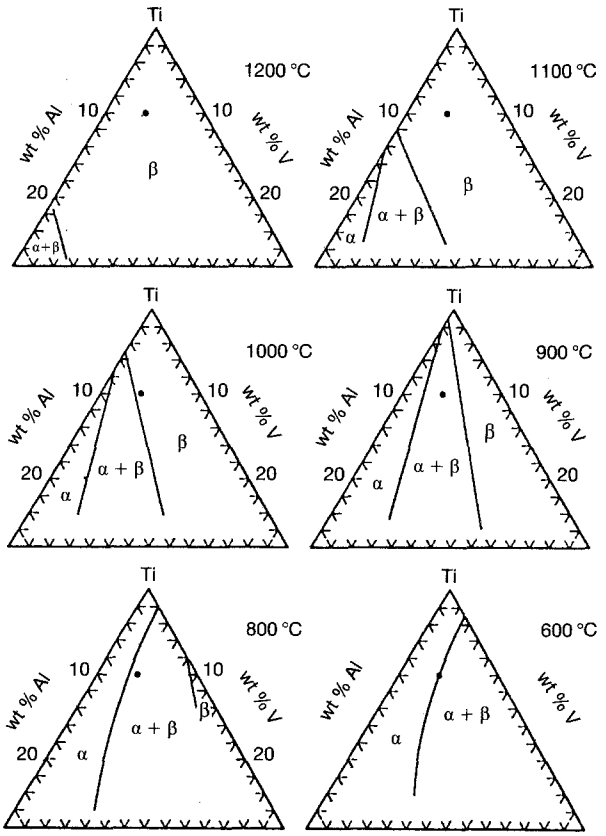

Figure 1 Ternary phase diagram of Ti–Al–V alloy. The solid circle indicate the alloy Ti–6Al–4V [15].

4.1 Solid solution strengthening

The effect of alloying elements added to Ti–6Al–4V is to produce solid solution strengthening. The important solid solution strengtheners for titanium alloys are the interstitial elements such as boron, nitrogen, carbon and oxygen and simple metals such as aluminium, gallium and tin [18]. Simple metals are basically substitutional α-stabilizer/strengtheners. On the other hand, β-stabilizer elements such as molybdenum, vanadium and zirconium cannot be regarded as solid solution strengtheners of titanium and its alloys.

4.1.1. Solid solution strengthening by α-stabilizers

When simple metals dissolved in titanium can form strong bonds between the solute and the surrounding titanium atoms, a moving dislocation will experience a strong pinning force and be stopped; therefore, alloy strength will increase. A synergistic effect was observed with the addition of ternary alloying elements in that they increased solid solution strengthening to a greater extent than binary additions.

4.1.2. Interstitial strengthening

In this group, boron, nitrogen, carbon and oxygen can be regarded as interstitial strengthening elements

[19, 20]. Their contribution to strengthening of titanium alloys is to distort the lattice by occupying the available interstitial sites in the crystal structure. Having close-packed hexagonal structure, α-phase can accommodate more interstitial atoms than β-phase that has a body-centred cubic structure. Thus interstitial strengthening for α-phase is quite important.

4.1.3. Solid solution strengthening by β-stabilizers

Solid solution strengthening due to the addition of β-stabilizers into titanium alloys is not as effective as in the case of α-stabilizers addition [18]. Although some degree of solution strengthening is introduced by β-stabilizer elements, the dominant strengthening for such alloys is precipitation strengthening.

4.2. Microstructural strengthening

The effectiveness of solid-solution strengthening does not extend far above room temperature. To extend the usable temperature range of titanium alloys, microstructural modification, including precipitation, is needed. Strengthening in such cases involves the following characteristic mechanisms: (i) direct interaction of dislocation with precipitate particles; (ii) coherency strains between matrix and second phase, (iii) coherency strains between matrix and precipitate. The aim of the present study was to harden the surface of Ti–6Al–4V alloy by laser surface melting alone and also by changing the surface composition with the addition of β stabilizer elements such as molybdenum, niobium and zirconium. To form the hard TiN, the laser processing was carried out in nitrogen atmosphere. Post-laser heat treatment was made to achieve additional hardening by microstructural modification, i.e., precipitation of nitrogen-base compounds and develop understanding of the hardness changes associated with temperature alteration.

5. Experimental procedure

The material investigated in this study was the commercial Ti–6Al–4V alloy. As-received material was cut and polished to obtain flat surfaces for laser processing. Laser surface melting and alloying experiments were carried out in a nitrogen gas atmosphere. In laser surface alloying, alloying elements, to be introudced into the melted layer, were in the form of thin foils with a thickness of 0.127 mm placed on the surface of the specimen. A GTE Sylvania Model 975 CO_2 gas transport laser, which provides a nominal output power of 5 kW continuous infrared radiation at a wavelength of 10.6 μm, was used. The beam diameter at the laser exit aperture is 45.7 mm and can be focused down to 0.5 mm through a focusing lens. The laser processing apparatus is shown in Fig. 2. The specimen is mounted on a rotating table, swept through the beam focused on the specimen surface. Approximately 2 cm^2 laser-melted or alloyed surfaces were obtained with an overlap of 50%. Following the laser processing, specimens were cut parallel to the laser beam raster direction. With suitable polishing and etching, melt depth and width as well as gross microstructural characterization were made through optical microscopy. A Vickers microhardness test was used to determine the hardness increments in laser surface melted and alloyed samples. X-ray diffraction analysis was used to identify the phases present after laser surface melting or alloying.

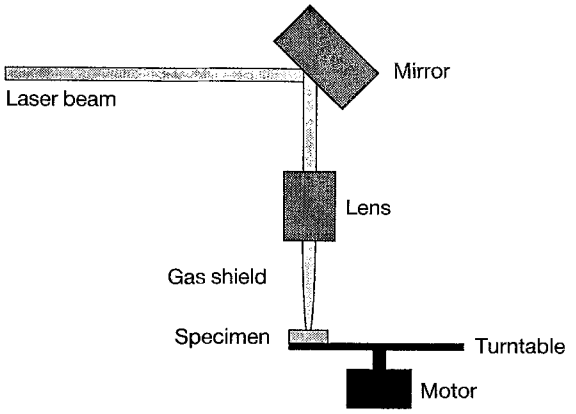

Figure 2 Laser processing apparatus.

6. Results and discussion

6.1. Laser surface melting of Ti–6Al–4V

Laser melting under a nitrogen gas atmosphere resulted in the formation of white dendrites covering the whole melted zone, the latter having a thickness of 750 μm (Fig.3). An X-ray diffraction pattern of the surface indicates the formation of TiN in the layer exhibiting high intensity TiN peaks with some low-intensity α-Ti peaks (Fig. 4a). This TiN formation on the surface, though not fully consistent with the actual VHN (1600 kg mm^{-2}) value of TiN, is still indicated to be present by the microhardness data shown in Fig. 5. VHN values of over 1000 were obtained in an area to a 100 μm depth from the surface. Hardnesses decreased to about 580 VHN at the end of the melted zone. Similar results are reported in the literature [13]. To understand the microstructural alteration of the low hardness regions, about 80% of the melted zone was polished away. The X-ray diffraction pattern of this surface revealed a decreasing TiN content and an increasing α-Ti content in the microstructure (Fig. 4b). Hardening in this region is believed to be due to the nitrogen solid solution effect. The presence of α-Ti in this region can be explained in terms of the high nitrogen content; because nitrogen is α stabilizer, as indicated earlier.

In the heat-affected zone (HAZ), hardness is fairly constant at about 450 VHN. During laser melting, the temperature at the HAZ can easily reach the β-phase field temperature. Rapid cooling from this field can cause martensitic transformation. The uniformity of hardness values in the HAZ seems to indicate the formation of hexagonal α′-Ti in this region.

To understand the hardening mechanisms operative in the melted zone, laser-melted samples were aged at 450 °C for different periods. Ageing for 1h increased

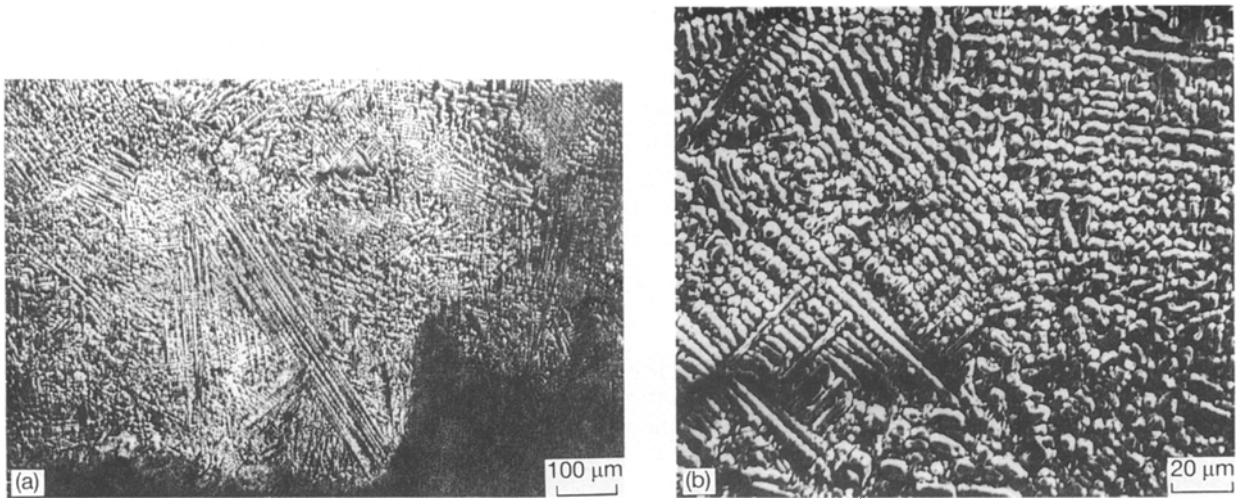

Figure 3 Laser surface melted structure of Ti–6Al–4V alloy, (a) from the melted zone, (b) showing dendritic structure.

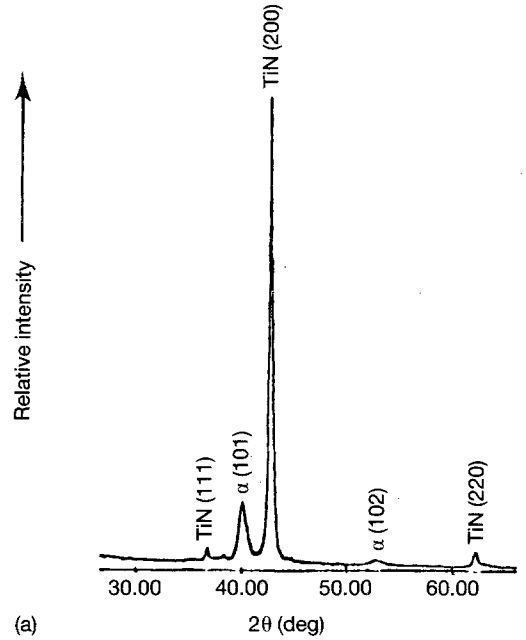

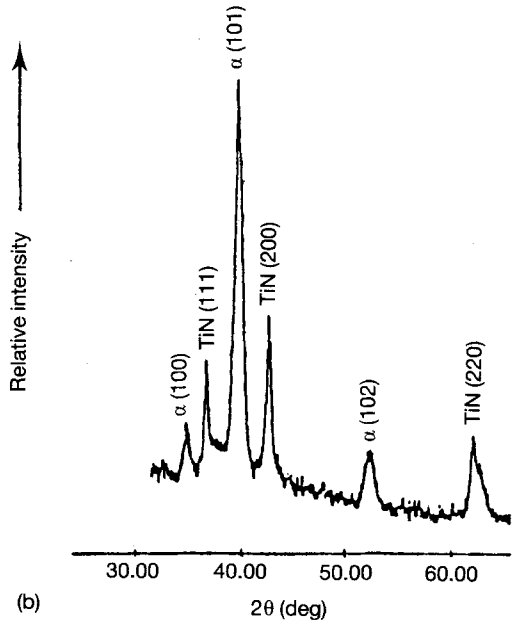

Figure 4 X-ray diffraction patterns of laser surface melted Ti–6Al–4V alloy (a) from the surface, (b) after 80% removal of the melted layer.

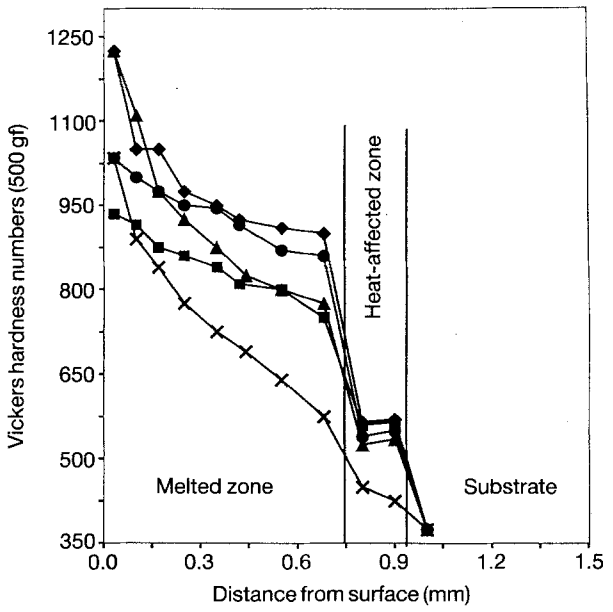

Figure 5 The hardness distribution of Ti–6Al–4V alloy which is laser surface melted under nitrogen gas aged at 450 °C and different ageing times. Power 5kW scan speed, 7mm s^{-1}. Ageing time (h) : (×) 0, (▲) 1, (◆) 3, (●) 7, (■) 20.

hardness by 20% in the melted zone. This might be due to the precipitation of Ti_2N, because excess nitrogen is present. Hardness in the HAZ also increased by 15%, reaching a constant value of 530 VHN. The increase in hardness in the HAZ is an indication of soft α′-Ti decomposition to relatively hard α + β phase mixture. Further ageing increased the hardness slowly; at the end of 20 h ageing, the hardness in the HAZ was about 570 VHN. This is consistent with the fact that, upon decomposition of α′, a stable α + β structure is produced.

After 20 h ageing, surface hardness decreased by 10% in comparison to the as-LSM sample. On the other hand, hardness distribution in the melted zone became almost uniform. As shown in Fig. 5, in the as-LSM sample, the hardness value at the bottom of the melted zone is around 45% less than that of the surface

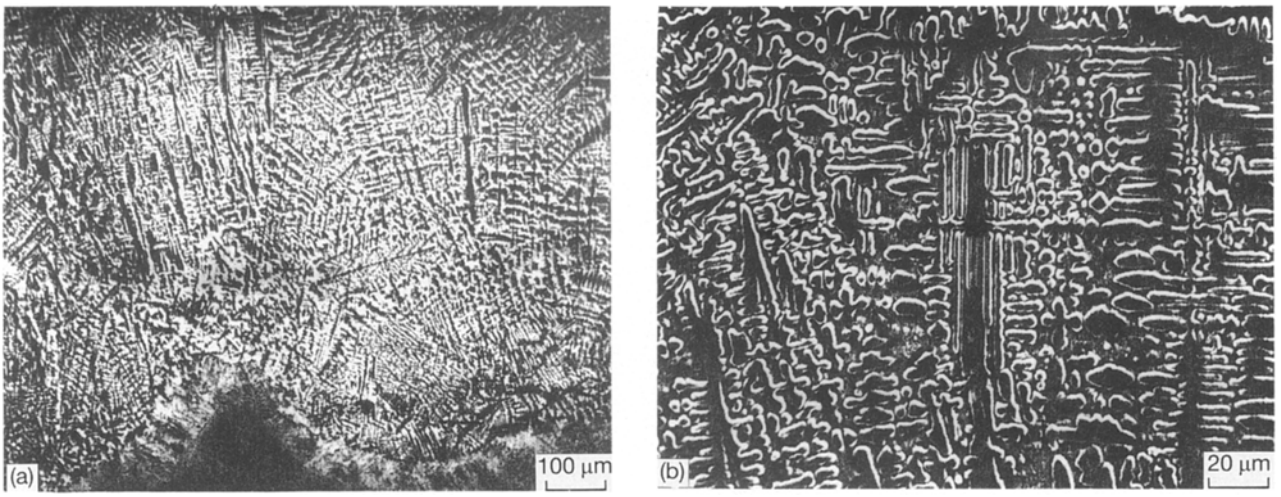

Figure 6 Laser surface melted structure of Ti–6Al–4V alloy after ageing 20 h at 450 °C, (a) from the melted zone, (b) showing disintegration of dendritic structure.

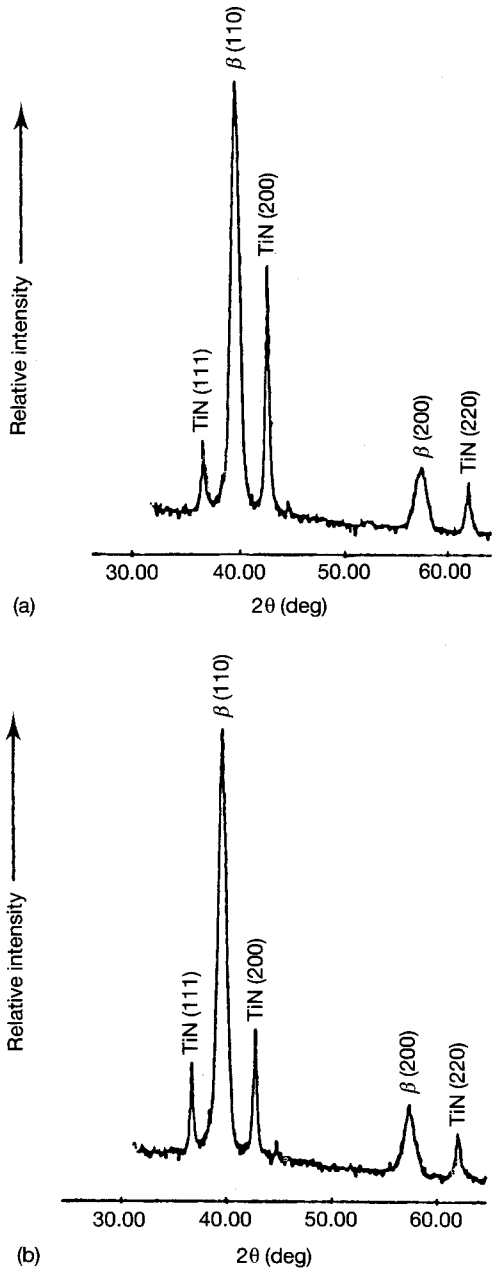

Figure 7 X-ray diffraction patterns of laser surface melted and molybdenum-alloyed Ti–6Al–4V, (a) from the surface, (b) after 80% removal of the melted layer.

hardness, but this difference is reduced to 16% after 20 h ageing treatment. Microstructure after 20 h ageing is shown in Fig. 6.

The observation of uniform hardness distribution in the melted zone after 20 h ageing can be attributed to the levelling out of nitrogen concentration by diffusion and to the precipitation of a Ti–N compound in the previously low hardness region. Diffusivity of nitrogen in α-Ti at 450 °C is calculated to be 3×10^{-15} cm^2 s^{-1} [21]. This diffusion rate of nitrogen affects the hardness, after 7 h ageing, by lowering the nitrogen concentration and thus the hardness by 20%. The lowering of hardness due to nitrogen diffusion, from the surface to the interior, becomes much more effective after 20 h ageing. This results with a 0.3 μm diffusion distance. A Ti–N compound precipitation is seen to start at the surface in short ageing times (i.e 1–3 h) because of the high nitrogen concentration there. However, this precipitation in the rest of the melted zone starts after the 3 h ageing treatment, as indicated by the increased hardness in these areas. The nature of the precipitating compounds will be elucidated in the near future with the completion of XRD studies.

The hardness profiles obtained suggest that the ageing contribution to the hardness change in the melted zone is the increased diffusivity of nitrogen that leads to a reduction of the solid-solution hardening effect of nitrogen at the surface, and precipitation of a stable Ti–N compound that increases the hardness throughout.

6.2. Laser surface alloying of Ti–6Al–4V

6.2.1. Molybdenum alloying

Molybdenum is known as a strong β stabilizer in titanium alloys [22]. X-ray diffraction analysis taken from the surface of the enriched samples shows that microstructure is dominated by β-phase and TiN (Fig. 7a). The microstructure of molybdenum alloyed Ti–6Al–4V is shown in Fig. 8. Molybdenum addition did not increase the hardness to a large extent in comparison with the as-LSM sample (Fig. 9). Also, the hardness distribution in melted zone seems to be fairly

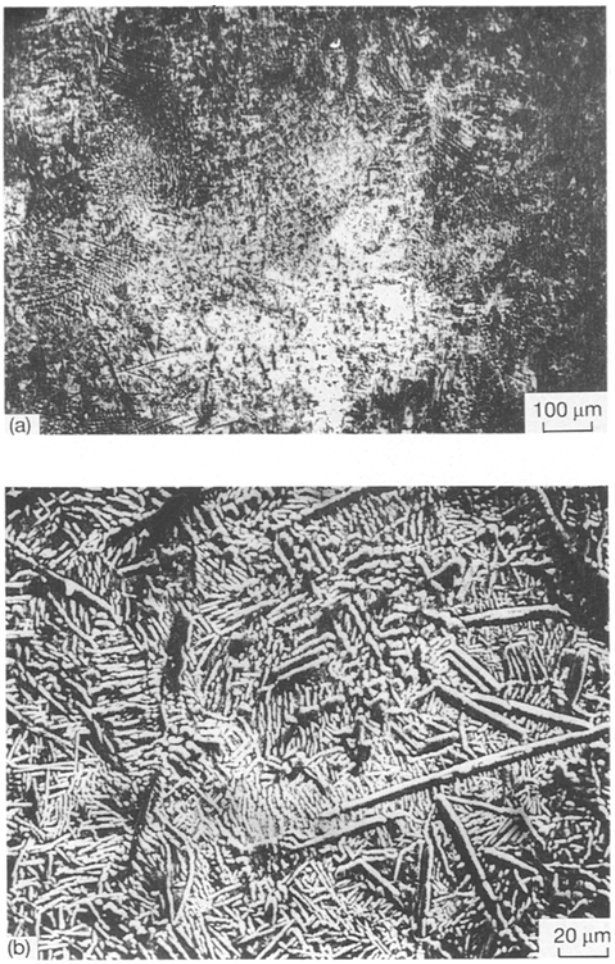

Figure 8 Laser surface molybdenum-alloyed structure of Ti–6Al–4V alloy, (a) from the melted zone, (b) showing dendritic structure.

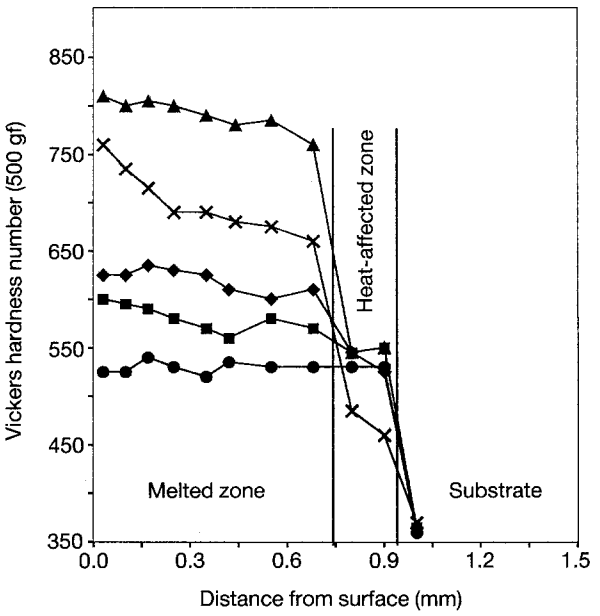

Figure 9 The hardness distribution of Ti–6Al–4V alloy which is laser surface melted and molybdenum alloyed under nitrogen gas, aged at 450°C and different ageing times. Power 5kW, scan speed, 7mm s^{-1}. Ageing time (h) : (×) 0, (▲) 1, (◆) 3, (●) 7, (■) 20.

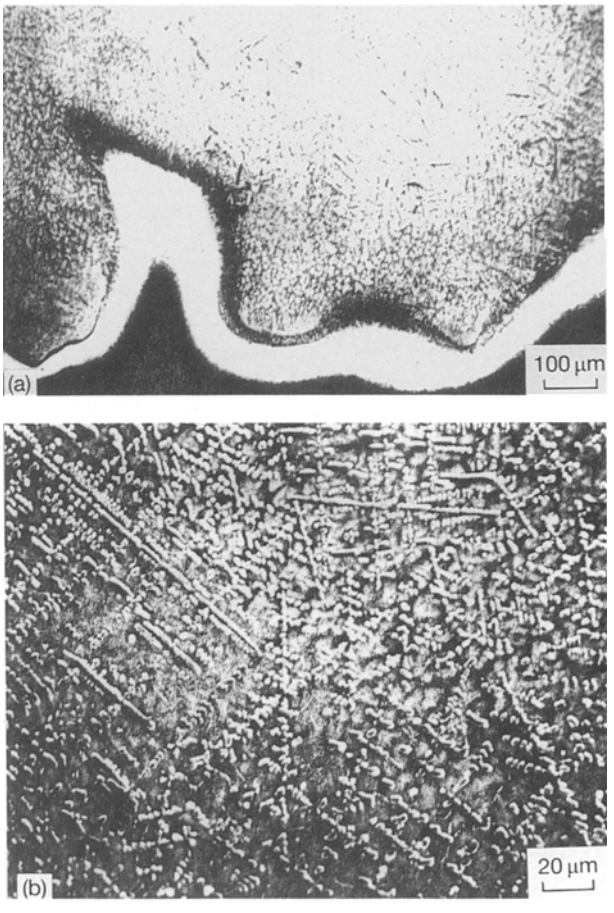

Figure 10 Laser surface molybdenum-alloyed structure of Ti–6Al–4V alloy after ageing 20 h at 450 °C, (a) from the melted zone, (b) showing disintegration of dendritic structure.

uniform. This is possibly due to the stability of β-phase as indicated by X-ray diffraction made after the removal of 80% of the melted zone (Fig. 7b).

Ageing treatments were performed for molybdenum alloyed samples as well. An ageing of 1 h increased hardness by 15% (Fig. 9). Hardness was very uniform in the melted zone. The increase in hardness is possibly due to the formation of hard, brittle ω-phase. This still remains to be verified with XRD. This phase is observed in β-Ti alloys, such as Ti–Mo, Ti–Nb, and Ti–V. It is formed either compositionally (athermal ω) or during heat treatment (isothermal ω) [23, 24].

However, further ageing (i.e. 7 h) decreased the hardness to that of the HAZ by dissolving hard ω-phase. Upon overageing (i.e. 20 h), α-phase precipitated and this, in turn, resulted in an increase in hardness. Fig. 10 shows the microstructure after 20 h ageing treatment. Some degree of recovery of the melted structure is observed in the well-defined grain-boundary formations and the disappearance of the dendritic structure. It suggests that additional hardness increase might be achieved if the ageing time is increased. The behaviour of the HAZ after laser alloying and ageing was identical to the LSM samples in terms of phase transformations and associated hardness changes.

The interesting observation from the hardness results is that a nitrogen solid solution strengthening effect is not seen to be present. This is very consistent with the low solubility of nitrogen in β-phase. Likewise, no contribution to the hardness due to a Ti–N compound precipitation is present after 20 h ageing treatment.

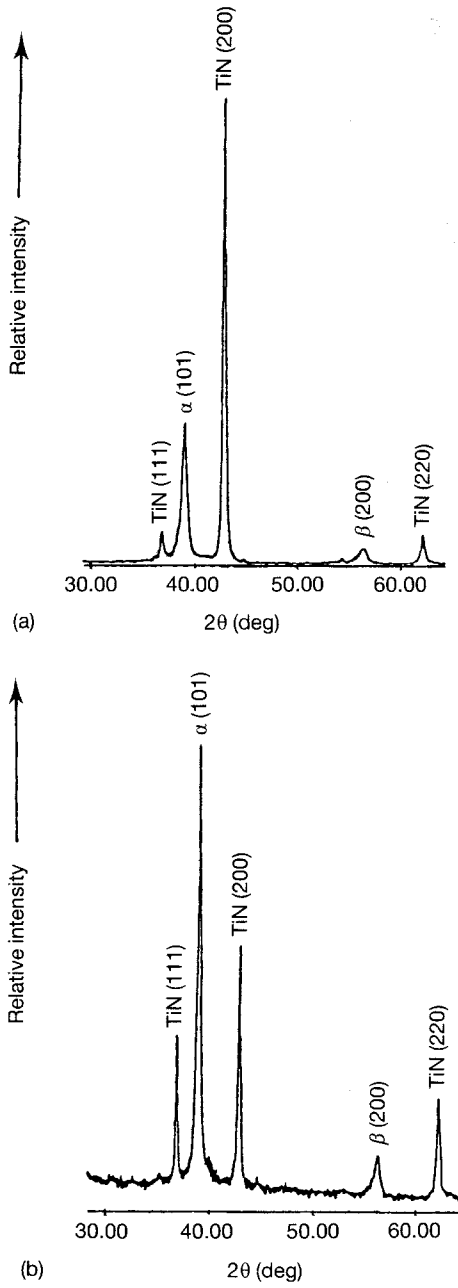

Figure 11 X-ray diffraction patterns of laser surface melted and nobium-alloyed Ti–6Al–4V, (a) from the surface, (b) after 80% removal of the melted layer.

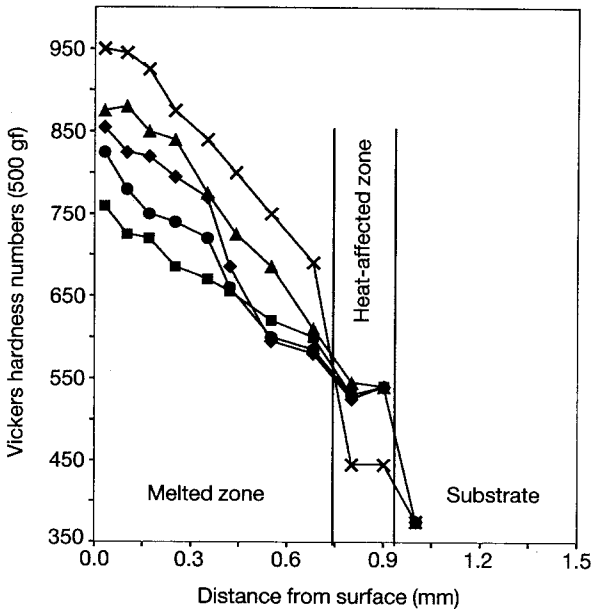

Figure 12 The hardness distribution of Ti–6Al–4V alloy which is laser surface melted and niobium alloyed under nitrogen gas is aged at 450 °C and different ageing times. Power 5 kW, scan speed, 7mm s^{-1}. Ageing time (h) : (×) 0, (▲) 1, (◆) 3, (●) 7, (■) 20.

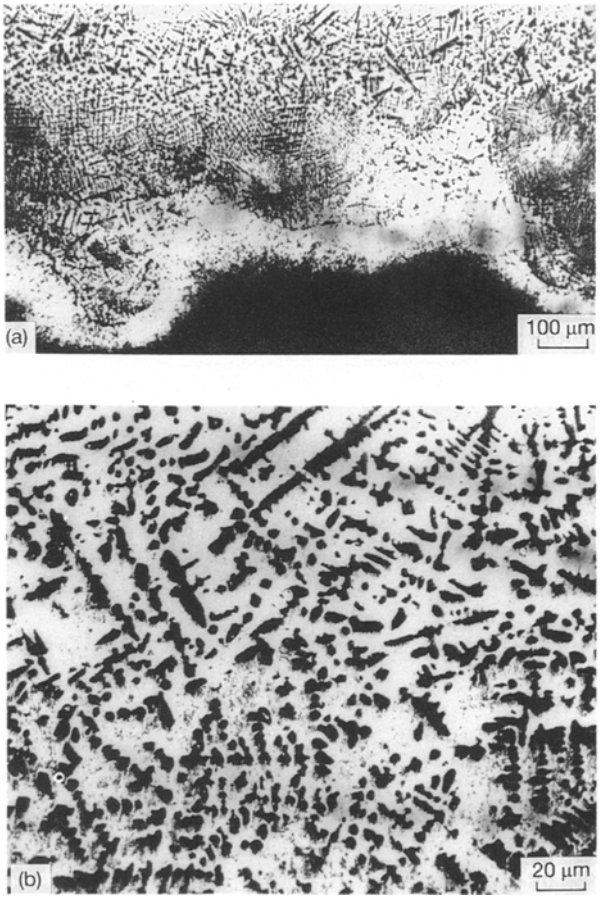

Figure 13 Laser surface niobium-alloyed structure of Ti–6Al–4V alloy, (a) from the melted zone, (b) showing dendritic structure.

6.2.2. Niobium alloying

Although niobium is recognized as a β stabilizer, X-ray diffraction shows that it is not as strong a β stabilizer as molybdenum. The high, intense peak observed with X-ray diffraction corresponds to TiN and not the β-phase (Fig. 11). In this case, it is clear that high surface hardness comes from the presence of TiN. Hardness decreases steadly to 700 VHN at the maximum melt depth (Fig. 12). Fig. 13 shows the microstructure of nibioum-alloyed Ti–6Al–4V.

Ageing treatments decreased hardness in the melted zone with increasing ageing times. Similar to the case of molybdenum alloying, niobium is expected to produce the hard ω-phase precipitation. Because this is not formed in the present process conditions, it seems likely that ω precipitation depends upon factors such as niobium concentration, ageing temperature, ageing time. An increased niobium concentration should increase the possibility of ω-phase formation, for short ageing times and lower ageing temperatures [25]. On the other hand, sufficiently long ageing times might

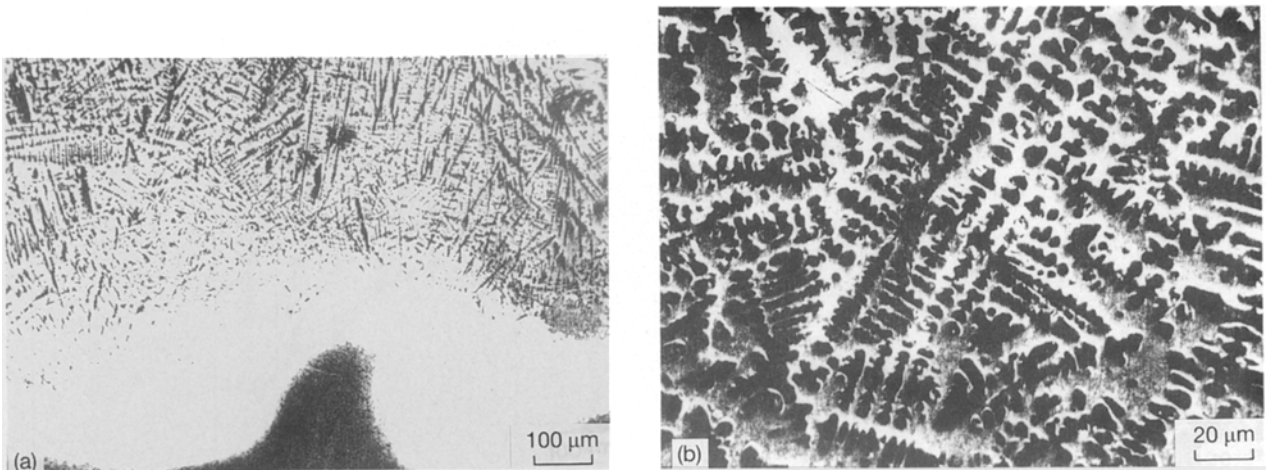

Figure 14 Laser surface niobium-alloyed structure of Ti–6Al–4V alloy after ageing 20 h at 450 ° C, (a) from the melted zone, (b) showing the disappearance of dendritic structure.

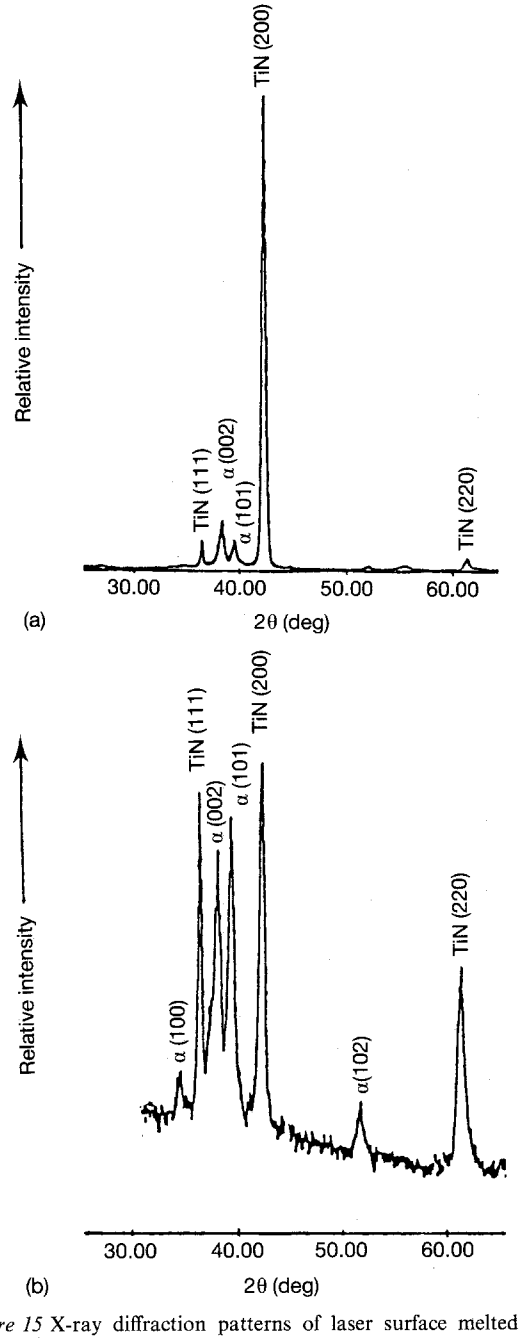

Figure 15 X-ray diffraction patterns of laser surface melted and zirconium-alloyed Ti–6Al–4V , (a) from the surface, (b) after 80% removal of the melted layer.

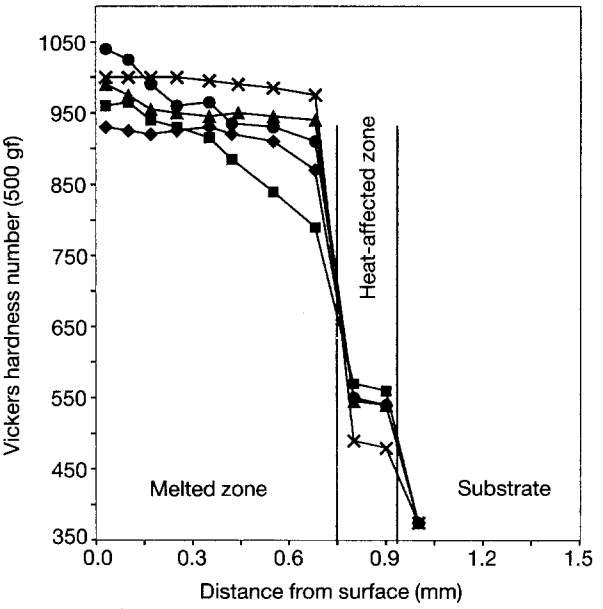

Figure 16 The hardness distribution of Ti–6Al–4V alloy which is laser surface melted and zirconium alloyed under nitrogen gas, aged at 450 °C and different ageing times. Power 5 kW; scan speed, 7mm s^{-1}. Ageing time (h) : (×) 0, (▲) 1, (◆) 3, (●) 7, (■) 20.

increase the hardness, as is observed in molybdenum alloyed samples, due to α-phase precipitation. Fig. 14 shows the microstructure after 20 h ageing.

The observed decrease in hardnesses at longer ageing times also imply the possibility of decreasing solid-solution strengthening effect of nitrogen. This was not observed in molybdenum alloyed samples.

6.2.3. Zirconium alloying

Zirconium has complete solid solubility in both β and α phases [26]. With the addition of zirconium to Ti–6Al–4V alloy, α-phase seems to become stable at ambient temperature due to the high cooling rate as well as the presence of nitrogen (Fig. 15a). Also, X-ray diffraction data taken, after removal of 80% of the alloyed layer, shows intense TiN and α-Ti peaks (Fig. 15b). Hardness in the alloyed zone was seen to be very uniform having about 1000 VHN value (Fig. 16).

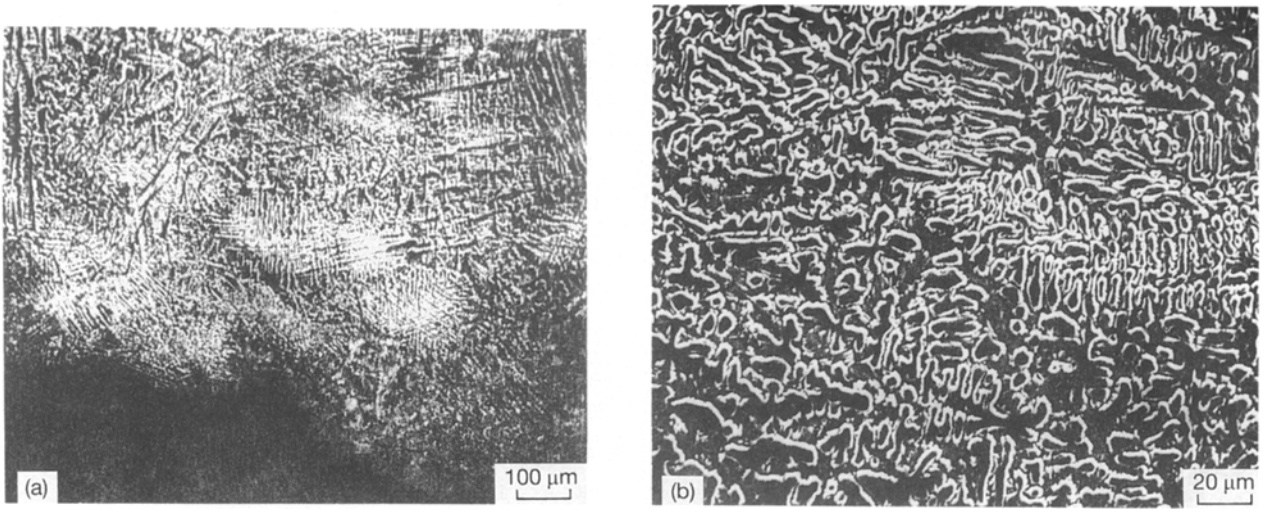

Figure 17 Laser surface zirconium-alloyed structure of Ti–6Al–4V alloy, (a) from the melted zone, (b) showing dendritic structure.

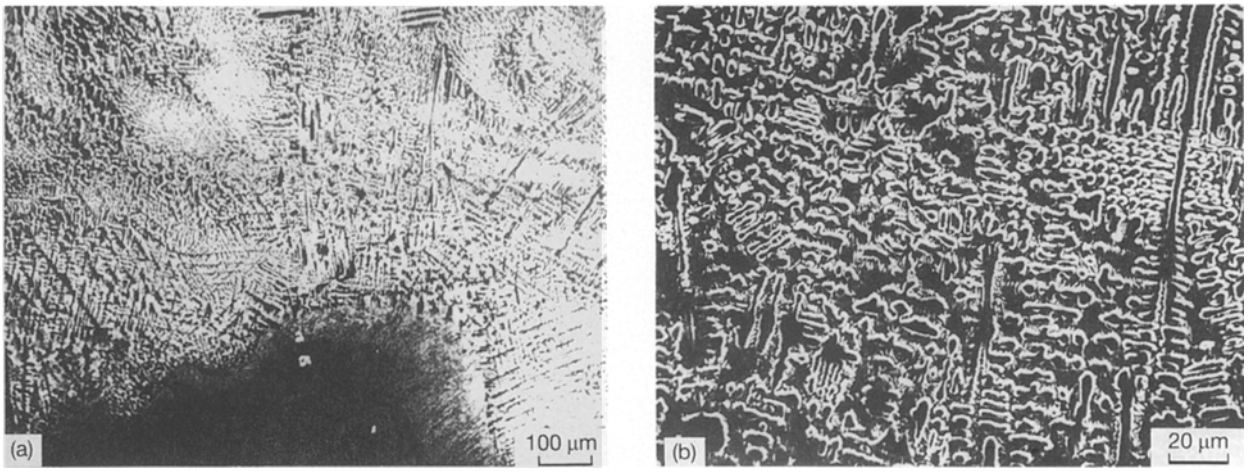

Figure 18 Laser surface zirconium-alloyed structure of Ti–6Al–4V alloy after ageing 20 h at 450 °C, (a) from the melted zone, (b) showing disintegration of dendritic structure.

After ageing for 7 h, hardness distribution did not change considerably, but further ageing (20 h) decreased hardness steadily. This behaviour, except for surface hardness, is very similar to that of a 20 h aged LSM sample, and once again, suggests a decreasing nitrogen solid solution strengthening effect to be the reason. Figs 17 and 18 show the microsture of a zirconium-alloyed sample, as-alloyed and after 20 ageing treatment, respectively. As expected, long ageing times remove the dendrites through solid state diffusion.

7. Conclusions

This study is an attempt to show that laser surface treatment, melting and alloying, of Ti–6Al–4V under a nitrogen gas atmosphere produces a hardened surface layer by TiN formation. The major conclusions may be summarized as follows.

1. Laser surface melting (LSM) alone, increased the surface hardness up to 1000 VHN. An ageing treatment of 20 h resulted in uniform hardness distribution in the melted zone.

2. Molybdenum and niobium addition did not increase the hardness as much as LSM alone. Ageing treatments reduced the hardnesses further.

3. The contribution of zirconium addition to the hardness is similar to LSM alone. Ageing treatments did not change the hardnesses considerably, and, more uniform hardness distribution was observed with zirconium addition.

4. The microstructure of the as-solidified heat-affected zone is α'-Ti for LSM and LSA and give the same hardness. Further ageing treatments increased hardness by the decomposition of α' and in the precipitation of $\alpha + \beta$ in the microstructure.

References

1. R. L. PREECE and K. W. J. BOWEN, *Met. Rev.* **22** (1961) 241.
2. A. D. McQUILLAN and A. K. McQUILLAN, "Titanium" (Academic Press, NewYork, 1956).
3. B. EDENHOFER, *Metal. Mater. Technol.* **8** (1976) 421.
4. "Metals Handbook", 9th Edn, Vol. 4 (ASM, Metals Park, OH, 1981) p. 213.
5. R. I. JAFFEE, H.R. OGDEN and D. J. MAYKUTH, *Trans. AIME* **188** (1950) 1261.

6. H. M. GABRIEL, F. SCHMIDT, E. BROSZEIT and K. H. KLOSS, *Thin Solid Films* **108** (1983) 189.
7. P. SIASHANSI, *J. Metals* **3** (1990) 30.
8. J. ZHANG, X. ZHANG, G. ZINTANG and L. HENGDE, *Mater. Res. Soc. Symp. Proc.* **55** (1986) 30.
9. S. KOU, D. K. SUN and Y. P. LEE, *Metall. Trans.* **14A** (1983) 643.
10. S. MANDZIEJ, M.C. SEEGERS and J. GODJIK, *Metal. Sci. Technol.* **5** (1989) 350.
11. J. R. BRADLEY and S. KIM, *Scripta Metall.* **23** (1989) 136.
12. Y. W. KIM, P. R. STRUTT and H. NOWOTNY, *Metall. Trans.* **10A** (1979) 881.
13. S. KATAYAMA, A. MATSUNAWA, A. MARIMOTO, S. ISHIMOTO and Y.ARATA, in "Laser Processing of Materials", edited by K. Mukherjee and J. Mazumder, (AIME, New York, 1985). p. 159.
14. J. D. AYERS, in "Lasers in Metallurgy", edited by K. Mukherjee and J. Mazumder, (AIME, New York, 1981) p. 115.
15. J. J. RAUSCH, F. A. CROSSLEY and H.D. KESSLER, *J. Metals* **8** (1956) 211.
16. C. HAMMOND and P. M. KELLY, in "Titanium Science and Technology and Application of Titanium", edited by R. I. Jafee and H. M. Burte (Pergamon Press, New York, 1970) p. 659.
17. J. C. WILLIAMS, *ibid.*, p.1433.
18. E. W. COLLINGS and H. L. GEDEL (eds), "Physics of Solid Solution Strengthening" (Plenum Press, New York, 1975) p. 147.
19. H. CONRAD, B. DeMEESTER, M. DONER and K. OKASAKI, in "Titanium Science and Technology and Application of Titanium", edited by R. I. Jaffee and H. N. Burte (Pergamon Press, 1970) p. 1.
20. H. CONRAD, *Progr. Mater. Sci.* **26** (1981) 123.
21. E: METIN and O. INAL, *Metall. Trans.* **20A** (1989) 1819.
22. R. A. WOOD, "Titanium Alloys Handbook", Metals and Ceramic Information Center, Battelle, Publication MCIC-HB-02 (1972).
23. H. E. COOK, *Acta. Metall.* **21** (1973) 1445.
24. *Idem, ibid.* **22** (1974) 239.
25. H. MARGOLIN and J. P. NIELSEN, in " Titanium Metallurgy in Modern Materials, Advances in Development and Applications ", vol. 2, edited by H. H. Hausner (Academic Press, (1960) p. 225.
26. B. S. HICKMAN, *Trans. TMS-AIME* **245** (1969) 1329.

Received 15 June 1992
and accepted 9 August 1993